Nuclear and Emerging Technologies for Space, American Nuclear Society Topical Meeting
Richland, WA, February 25 – February 28, 2019, available online at http://anstd.ans.org/

DEVELOPMENT OF SINTERED YTTRIUM DIHYDRIDE COMPACTS FOR NUCLEAR REACTOR MODERATOR APPLICATIONS

A.P. Shivprasad[1*], J.R. Wermer[2], T.A. Saleh[1], J.T White[1], E.P. Luther[2], and D.V. Rao[3]

[1]*Materials Science and Technology, Los Alamos National Laboratory, Los Alamos, NM, 87545, aps@lanl.gov*
[2]*Sigma Division, Los Alamos National Laboratory, Los Alamos, NM, 87545*
[3]*Civilian Nuclear Programs, Los Alamos National Laboratory, Los Alamos, NM, 87545*

High-density compacts of yttrium dihydride were synthesized using powder metallurgy and exhibited densities greater than 90% of the theoretical density. Compacts were then examined for phase purity using X-ray diffraction and elastic properties using resonant ultrasound spectroscopy. Results showed that sintered material was made up of approximately 1% yttrium trihydride and the rest yttrium dihydride. Young's, bulk, and shear moduli were all lower than reported in literature and were attributed to internal porosity. Modulus values were clearly observed to vary as functions of density, while Poisson's ratio was calculated as 0.221 ± 0.003 and was independent of density. This work represents a novel achievement in demonstrating the feasibility of powder processing techniques to yield high-density yttrium dihydride compacts.

I. INTRODUCTION

Current generation nuclear plants are ill-suited for adaptation to space applications to enable long-duration crewed missions to outer planetary bodies. Very small modular reactors (vSMRs) – owing to their small size, low capital cost, and low power – could address these demands[1,2]. In particular, vSMRs could be designed to be inherently self-regulating such that reactor power may be varied to reflect power needs without requiring active controls or a number of on-site operators. One proposed vSMR is a high-temperature reactor that uses heat pipe technology to cool the reactor core and metal hydrides as the moderator due to their high hydrogen density[3]. Use of a hydrogenous moderator to thermalize neutrons enhances the fuel utilization and cost-effectiveness of vSMRs while keeping the core portable.

Yttrium dihydride (YH_2) is a promising candidate metal hydride for this application due to its high thermal stability and good mechanical properties for a rare earth hydride[4–6]. Despite these advantages, it is difficult to produce hydride monoliths in geometries required for reactor design concepts.

Challenges in producing yttrium dihydride monoliths in complex geometries is due to the inherent materials challenges associated with hydriding. (1) The hydrogen absorption reaction is associated with accommodation of hydrogen atoms into the interstitial sites of the metal sublattice, resulting in a significant volume expansion and embrittlement[6]. (2) Hydride formation by direct reaction between metal and hydrogen gas is typically done in evacuated, isolated vessels with strict pressure control to ensure product purity[7]. Because of the issues accompanying the production of large-scale, leak-free hydrogen pressure vessels, large, complex shapes of metal hydrides are difficult to fabricate using direct hydriding methods.

To that end, it is of great interest to explore alternate production paths for metal hydride monoliths to alleviate the issues presented by direct hydriding methods. One such pathway is powder metallurgy, whereby a pre-hydrided metal is crushed into a powder, pressed into a specified shape, and then sintered into a high-density compact.

In this study, yttrium dihydride compacts were fabricated using powder metallurgical methods. Sintered pellets were then analyzed for elastic moduli using resonant ultrasound spectroscopy (RUS).

II. EXPERIMENTAL METHODS

II.A. Hydride synthesis

Bulk yttrium dihydride was synthesized by direct hydriding of high-purity yttrium metal in a Sieverts' apparatus[7]. Trace element analysis was performed using inductively coupled plasma mass spectrometry (NSL Analytical Services, Cleveland, OH); results are summarized in **Table I**.

Table I. Trace element contents (in weight ppm) of Y metal used in this study. Contents are reported for tantalum, transition metals (TM) excluding Ta and Y, rare earth (RE) metals, and other elements (alkaline earth metals, alkali metals, other metals, non-metals, and metalloids, in order of concentration).

Element	Ta	TM (excl. Y, Ta)	RE metals	Other
Composition (wt. ppm)	2400	430	130	470

Metal samples were placed onto molybdenum foils and loaded into a quartz reaction vessel, which was then attached to a gas manifold and placed inside a tube furnace.

All gas manifold connections were composed of VCR (Swagelok) fittings using silver-plated nickel gaskets to provide a leak-tight seal.

Hydrogen dosing was performed between 1083 and 1103 K by slowly aliquoting hydrogen over period of 6-8 days. The final product was a brittle, air-stable solid that was able to be dry-machined. Final stoichiometry was calculated using the ideal gas law and mass gain and corresponded to an H/Y atom ratio of 1.8. Hydrogen content was also measured using inert gas fusion[8] (ASTM E1447-09, LUVAK Inc, Boylston, MA, USA) as 2.04 wt. %, corresponding to an H/Y ratio of 1.85. An example monolith formed by direct hydriding is shown in **Fig. 1**.

Fig. 1. Image of 1-inch-diameter YH_2 monolith showing examples of dry-machining on the upward-facing side.

II.B. Phase evaluation

Phase contents of the initial hydride feedstock and sintered pellets were investigated using a Bruker D2 X-ray Diffractometer (XRD, Bruker, Wisconsin, USA). Feedstock material and sintered pellets were fractured in an inert glovebox line to generate approximately 50-mg fragments. These fragments were then ground to powder using a mortar and pestle and then sealed in an XRD sample holder using vacuum grease and a polymer dome with an air-scatter shield to reduce X-ray background at low angles. XRD scans were performed from 25° to 40° 2θ with a scan resolution of 0.01° 2θ and a live time of 5-s per angular step. These scan parameters were chosen to correspond with the maximum-intensity peaks of the yttrium dihydride powder diffraction file (PDF) and also capture the maximum-intensity peaks for secondary phases such as yttrium trihydride and yttrium oxide.

II.C. Powder processing and sintering

Monoliths of yttrium dihydride were broken into small pieces and then introduced into a high-purity argon glovebox line for further size-reduction. Masses on the order of 1-g were crushed using a high-energy ball mill (8000M, SPEX Sample Prep, USA) with 0.25 wt. % ethylene bis(stearamide) (EBS) binder for 30 minutes and subsequently sieved through a 325-mesh sieve (sub-44-μm mean particle size). Pellets of yttrium dihydride were pressed at 150 MPa using a 5.2-mm diameter punch and die set. Green bodies were then sintered for 10-hours in a tungsten-mesh furnace. Final dimensions of sintered pellets were measured to determine the geometric density with respect to the theoretical density of yttrium dihydride (4.28-g/cm^3). Density values were also measured using Archimedes method[9] (ASTM B962-17).

II.D. Resonant ultrasound spectroscopy (RUS)

RUS measurements were made at constant amplitude using a National Instruments NI, PXIe 1075 function generator. Generation and acquisition lines were managed by the Resonance Inspection Techniques and Analysis (RITA©) software package developed at LANL (Ref. 10). **Fig. 2** shows the experimental setup used in this study.

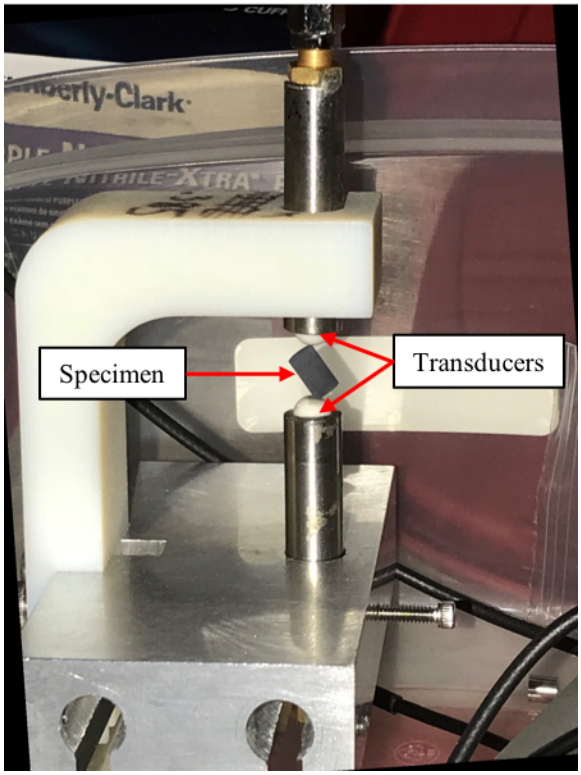

Fig. 2. Experimental setup for a cylindrical RUS sample placed between hemispherical Al_2O_3 wear plates, glued to transducers.

The driving frequency was varied between 300 to 800 kHz. The corners of each sample were positioned in transducers to reduce symmetry effects (as in **Fig. 2**). Elastic constants were calculated from a spectrum using the Rayleigh-Ritz method from the resonance frequencies[11,12]. The model depended on sample mass and dimensions and a numerical approximation was used to iteratively fit elastic constants[11].

Three sintered pellets of yttrium dihydride were analyzed using RUS. For each sample, 30-50 resonances were obtained and inversion was within 0.5% root mean square (RMS) error. Assuming each sample was comprised of a polycrystalline, isotropic material, the independent moduli are C_{11} and C_{44}. From these two values, the shear

(G), bulk (K), and Young's (E) moduli, as well as Poisson's ratio (ν) were calculated as follows:

$$G = C_{44} \quad (1)$$

$$K = C_{11} - \frac{4}{3}C_{44} \quad (2)$$

$$E = C_{11} - \frac{2\,(C_{11} - 2C_{44})^2}{2\,(C_{11} - C_{44})} \quad (3)$$

$$\nu = \frac{C_{11} - 2C_{44}}{2\,(C_{11} - C_{44})} \quad (4)$$

III. RESULTS AND DISCUSSION

III.A. Powder processing and sintering

A summary of masses and densities of sintered yttrium dihydride compacts is shown in **TABLE II**, which illustrates that sintered pellets had densities between 90 and 95% of the theoretical density of yttrium dihydride. **Fig. 3** shows (A) an example image of a sintered compact and (B) a corresponding optical micrograph.

TABLE II. Summary of geometric (G) and immersion (I) density measurements of YH_2 sintered pellets. Results are compared with the theoretical density (TD) of YH_2. Bold samples were also examined using RUS.

Sample	% TD (G)	% TD (I)
1	94.18	93.85
2	**94.79**	**94.30**
3	**94.37**	**94.08**
4	**91.25**	**90.49**
5	93.12	94.90
6	89.82	90.40

Previous work on metal hydride powder metallurgy had suggested that compacts of metal hydrides would be unfeasible due to the low density of pressed compacts and the difficulty of sintering due to potential pulverization from the inability to sinter[12]. In the literature, this drawback was offset by using a metal matrix[12], by sintering metal compacts in pure hydrogen[13], or by arc-melting green bodies with metal powder additives[6]. The work presented here has shown that powder metallurgy of yttrium hydride without pulverization or dehydriding during sintering yields high-density sintered compacts.

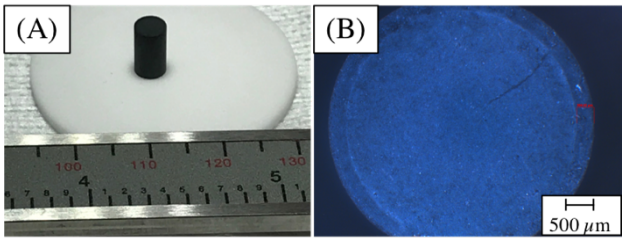

Fig. 3. Image of 94% dense, sintered YH_2 pellet. (A) Photo of YH_2 sintered pellet taken using a camera. Ruler included to show scale. (B) Dark-field optical micrograph of as-fabricated, circular cross-section of pellet. Sample surface shows a scratch due to handling with tweezers.

III.B. Phase purity of material

Monoliths of yttrium dihydride formed by direct-hydriding in the Sieverts' apparatus and sintered pellets were both analyzed for phase purity using XRD. Diffraction patterns for both materials are shown in **Fig. 4**.

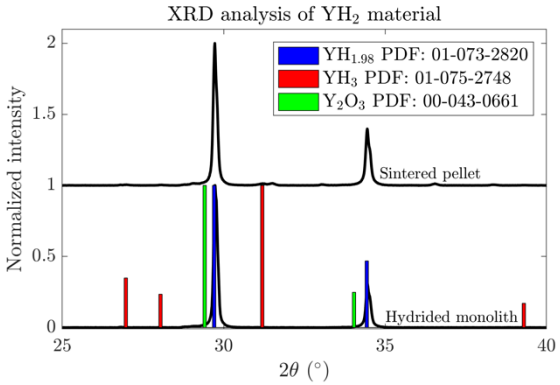

Fig. 4. XRD patterns obtained from the hydrided monolith and the sintered pellet. Patterns were compared with PDF indices for $YH_{1.98}$ (PDF #01-073-2820), YH_3 (PDF #01-075-2748), and Y_2O_3 (PDF #00-043-0661). Remaining peaks were identified to be due to other Y-containing oxide phases.

Fig. 4 plots XRD pattern intensity as a function of 2θ for yttrium dihydride hydrided in the Sieverts' apparatus, yttrium dihydride sintered pellets, and the PDF peak indices for yttrium dihydride, yttrium trihydride (YH_3), and yttrium(III) oxide (Y_2O_3). Comparison of the pattern for Sieverts'-produced yttrium dihydride with the PDF peak indices shows that the hydrided material was phase-pure yttrium dihydride. A similar comparison for the pattern acquired from the sintered compact indicates that it was not phase-pure yttrium dihydride, but was approximately 1% yttrium trihydride. It was experimentally determined that the trihydride formed during the high-energy ball-milling step of powder processing or due to residual hydrogen from the sintering step, as the increased temperatures during these steps are able to cause phase transformations in the presence of hydrogen [4,14]. Although only trace amounts of hydrogen were present in the inert glovebox line used for powder processing, the pressures of hydrogen required to form the trihydride from the dihydride at lower temperatures (< 200 °C) are low (< 30 torr) (Ref. 14) and the high surface areas associated with powders drastically improved the kinetics of transformation.

III.C. Mechanical properties of yttrium dihydride

Fig. 5 shows an example resonance spectrum obtained from sintered yttrium dihydride and plots resonance magnitude as a function of frequency. These frequencies

may include singlet, doublet, and multiplet peaks which were then indexed and fit to a function using elastic constants as fitting parameters. Error was calculated as the deviation from theoretical values based on geometry and mass.

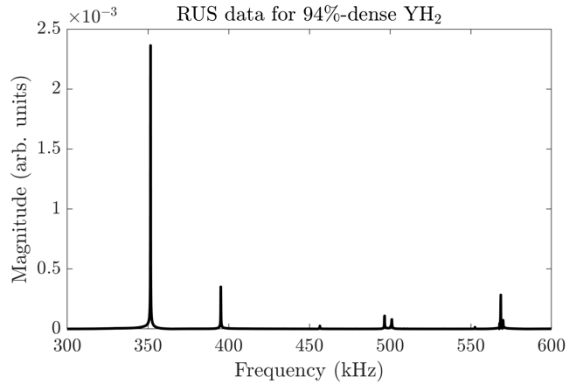

Fig. 5. Measured frequency response of a sintered YH_2 pellet. Frequency shown here between 300 and 600 kHz.

Elastic constants, C_{11} and C_{44}, and the associated RMS values are shown in **Table III**. The data presented here shows a clear effect of density on the measured values.

Table III. Elastic constants for yttrium dihydride determined from this study. Values are shown with 95% confidence intervals.

#	% TD (I)	C_{11} (GPa)	C_{44} (GPa)	RMS error (%)
2	94.30	133.0 ± 1.2	47.6 ± 0.4	0.470
3	94.08	125.8 ± 1.2	44.7 ± 0.4	0.440
4	90.49	113.4 ± 0.6	41.0 ± 0.2	0.261

Elastic constants were calculated as described in Eq. (1) - (4). A plot of these values as functions of percent theoretical density is shown in **Fig. 6**. Poisson's ratio was found to be independent of density and was calculated as ν = 0.221 ± 0.003 (±95% CI). Poisson's ratio was also calculated from literature values and was found to be 0.231 (Ref. 15).

Fig. 6 shows a general trend of increasing elastic moduli as a function of density from the collected data points (empty circles). The data from this study are compared with those of literature values using sound velocity techniques[15]. These values were determined based on maintaining the same stoichiometry as the yttrium dihydride from this study (H/Y = 1.85) and assuming 100% the theoretical density; data for stoichiometry was interpolated from linear fits in the literature.

If a sintered pellet is considered as a mixture between yttrium dihydride and void, then it is possible to use the rule of mixtures to calculate the expected values of the moduli given the density of the sintered compact. This is done in **Table IV** for Young's Modulus. This result shows clearly that the rule of mixtures does not completely explain the difference between the literature values and those obtained from this study. This could be due to the ~1% yttrium trihydride in the pellet, as determined using XRD. However, only values for bulk moduli of the trihydride exist in literature and there is a large variation among sources (factor of two difference), though all are higher than that of the dihydride here and in other studies [16,17].

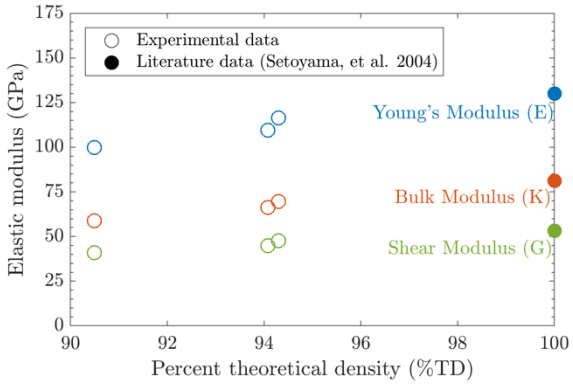

Fig. 6. Elastic moduli of YH_2 sintered compacts calculated from RUS results. Data are plotted as a function of immersion density in terms of percent theoretical density. Data points from literature are also plotted for the given stoichiometry and an assumed density of 100% the theoretical density. Error bars from **Table III** are too small to observe in this plot.

Table IV. Summary of elastic constants of YH_2 measured in this study and compared with a rule of mixtures calculation based on values in the literature[15].

#	% TD (I)	E_{meas} (GPa)	E_{calc} (GPa)	ΔE (GPa)
2	94.30	116.3	122.6	6.9
3	94.08	109.5	122.3	13.2
4	90.49	99.7	117.6	18.9

IV. II. CONCLUSIONS

High-density compacts of yttrium dihydride were sintered from pre-hydrided metal and then examined for pellet density and elastic constants. Key conclusions are summarized below:

1. Sintered pellets exhibited densities close to or above 90% for both geometric and immersion densities.
2. The phase composition of sintered pellets was very close to phase-pure, with approximately 1% of the material as yttrium trihydride. This was found to be due to the ball-milling process in the presence of trace amounts of hydrogen.

3. Elastic constants were found to depend on compact density and were lower than values reported in literature. This was partially attributed to the internal porosity and the small amount of the trihydride in the compacts.

The findings in this study demonstrate the feasibility of high-density sintered components of yttrium hydride and represent a significant technical advancement for metal hydride applications in nuclear reactors. Future work will focus on further studying the effect of porosity on properties and will measure thermal properties, such as thermal conductivity and thermal expansion, of sintered pellets.

V. ACKNOWLEDGMENTS

The authors would like to thank Dustin Cummins of LANL for helpful discussions regarding the sintering studies. The authors would also like to thank John Dunwoody and Chris Grote for their invaluable technical support. Finally, the authors would like to thank the LANL Lab Directed Research and Development program for supporting this research. This work was partially funded by the USDOE Office of Nuclear Energy (NE).

VI. REFERENCES

1. J. VUJIĆ et al., "Small modular reactors: Simpler, safer, cheaper?," Energy **45** 1, 288 (2012); https://doi.org/https://doi.org/10.1016/j.energy.2012.01.078.
2. J. L. ANDERSON JR, E. LANTZ, and W. MAYO, "Reactivity control of fast-spectrum reactors by reversible hydriding of yttrium zones" (1968).
3. M. A. GIBSON et al., "NASA's Kilopower Reactor Development and the Path to Higher Power Missions," 20170011067 (2017).
4. L. N. YANNOPOULOS, R. K. EDWARDS, and P. G. WAHLBECK, "The Thermodynamics of the Yttrium-Hydrogen System1," J. Phys. Chem. **69** 8, 2510 (1965); https://doi.org/10.1021/j100892a004.
5. C. E. LUNDIN and J. P. BLACKLEDGE, "Pressure-Temperature-Composition Relationships of the Yttrium-Hydrogen System," J. Electrochem. Soc. **109** 9, 838 (1962); https://doi.org/10.1149/1.2425565.
6. J. P. BLACKLEDGE, "CHAPTER 1 - An Introduction to the Nature and Technology of Hydrides," in Metal Hydrides, W. M. Mueller, J. P. Blackledge, and G. G. Libowitz, Eds., pp. 1–20, Academic Press (1968); https://doi.org/10.1016/B978-1-4832-3215-7.50005-8.
7. R. CHECCHETTO, G. TRETTEL, and A. MIOTELLO, "Sievert-type apparatus for the study of hydrogen storage in solids," Meas. Sci. Technol. **15** 1, 127 (2004); https://doi.org/10.1088/0957-0233/15/1/017.
8. "ASTM E1447 - 09, Standard Test Method for Determination of Hydrogen in Titanium and Titanium Alloys by Inert Gas Fusion Thermal Conductivity/Infrared Detection Method," ASTM International, West Conshohocken, PA (2016); https://doi.org/10.1520/e1447-09r16.
9. "ASTM B962 - 17, Standard Test Methods for Density of Compacted or Sintered Powder Metallurgy (PM) Products Using Archimedes' Principle," ASTM International, West Conshohocken, PA (2017); https://doi.org/10.1520/b0962-17.
10. C. PAYAN et al., "Quantitative linear and nonlinear resonance inspection techniques and analysis for material characterization: Application to concrete thermal damage," The Journal of the Acoustical Society of America **136** 2, 537 (2014); https://doi.org/10.1121/1.4887451.
11. U. CARVAJAL-NUNEZ et al., "Determination of elastic properties of polycrystalline U3Si2 using resonant ultrasound spectroscopy," Journal of Nuclear Materials **498**, 438 (2018); https://doi.org/https://doi.org/10.1016/j.jnucmat.2017.11.008.
12. M. RON et al., "Preparation and properties of porous metal hydride compacts," Journal of the Less Common Metals **74** 2, 445 (1980); https://doi.org/10.1016/0022-5088(80)90183-6.
13. J. HUOT, H. HAYAKAWA, and E. AKIBA, "Preparation of the hydrides Mg2FeH6 and Mg2CoH5 by mechanical alloying followed by sintering," Journal of Alloys and Compounds **248** 1, 164 (1997); https://doi.org/https://doi.org/10.1016/S0925-8388(96)02705-3.
14. O. SOROKA et al., "Control of YH3 formation and stability via hydrogen surface adsorption and desorption," Applied Surface Science **455**, 70 (2018); https://doi.org/10.1016/j.apsusc.2018.05.134.
15. D. SETOYAMA et al., "Mechanical properties of yttrium hydride," Journal of Alloys and Compounds **394** 1, 207 (2005); https://doi.org/10.1016/j.jallcom.2004.10.035.
16. T. PALASYUK and M. TKACZ, "Hexagonal to cubic phase transition in YH3 under high pressure," Solid State Communications **133** 7, 477 (2005); https://doi.org/10.1016/j.ssc.2004.11.035.
17. A. MACHIDA et al., "X-ray diffraction investigation of the hexagonal–fcc structural transition in yttrium trihydride under hydrostatic pressure," Solid State Communications **138** 9, 436 (2006); https://doi.org/10.1016/j.ssc.2006.04.011.